Structure-Rheology Responses of Polylactide/Calcium Carbonate Composites

Shu-Ying Gu,[1,2] Cun-Yang Zou,[1] Kai Zhou,[1] Jie Ren[1,2]

[1]*Institute of Nano and Bio-Polymeric Materials, School of Materials Science and Engineering, Tongji University, Shanghai 200092, China*
[2]*Key Laboratory of Advanced Civil Engineering Materials, Ministry of Education, School of Materials Science and Engineering, Tongji University, Shanghai 200092, China*

Received 15 February 2009; accepted 17 May 2009
DOI 10.1002/app.30768
Published online 23 June 2009 in Wiley InterScience (www.interscience.wiley.com).

ABSTRACT: Polylactide (PLA) and calcium carbonate ($CaCO_3$) were melt blended using a twin-screw extruder. The morphology of PLA/$CaCO_3$ composites was observed by scanning electronic microscopy. The linear and nonlinear shear rheological behaviors of PLA/$CaCO_3$ melts were investigated by an advanced rheology expended system. The results show that the $CaCO_3$ particles are evenly dispersed in the PLA matrix. The incorporation of low $CaCO_3$ content (<20%) causes the reduction of the storage moduli, loss moduli, and dynamic viscosities whereas high $CaCO_3$ content (>30%) leads to the increase of the storage moduli, loss moduli, and dynamic viscosities. The composites with high $CaCO_3$ content show pseudo-solid-like behaviors at low frequency. High $CaCO_3$ content also results in a significant increase of flow activation energy and a dramatic decrease of flow index *n*, which is in consistent with the more serious shear-thinning tendency of high-filled PLA composites melts. The particular rheological responses might be attributed to the formation and destruction of the percolating network. © 2009 Wiley Periodicals, Inc. J Appl Polym Sci 114: 1648–1655, 2009

Key words: rheology; viscoelastic properties; structure; polylactide; calcium carbonate

INTRODUCTION

Polylactide (PLA) is one of the most important environment-friendly biodegradable thermoplastic polyester with extensive application.[1] Because of its renewable resources and excellent mechanical properties comparable with many petroleum-based plastics, much attention has been paid for its use in service ware, grocery, waste-composting bags, mulch films, and controlled release matrices.[2] However, some of its properties such as poor impact strength, low heat distortion temperature and higher price prevent its application in some fields. In spite of these difficulties, many considerable efforts have been made to improve the properties of PLA in order that it can compete with low cost, flexible commodity polymers. Until now much work has been concentrated on PLA/clay nanocomposites[3–6] and its blends with flexible polymers, such as poly(ε-caprolactone), poly(ethylene glycol), poly (butylenen adipate-co-terephthalate), and poly (butylene succinate).[7,8]

Incorporation of various mineral fillers into PLA is one of the simplest and most cost-effective ways to improve the properties of PLA. The properties of the resulting composites are determined by the particle size and size distribution, shape, modulus, content and dispersion of filler in the polymer matrix. The interactions between the filler particles as well as filler particles and polymer matrix also have significant impact on the properties of the composites. Typical mineral fillers with different shape and size including calcium carbonate ($CaCO_3$), calcium phosphate ($Ca(H_2PO_4)_2$), calcium sulfate ($CaSO_4$), talc, and mica were incorporated into PLA.[9–11] $CaCO_3$ is traditionally used in plastics as bulking agent because of its wide range of application and low cost. Modern technologies have been developed to prepare nanosized $CaCO_3$ with special shapes and a narrow size distribution. Furthermore, many kinds of surface modifiers such as stearic acid, silanes, titanates, and zirconates have been used to reduce the high-surface energy to avoid particle agglomeration.[12] It has been proven to be an effective way to

Correspondence to: S.-Y. Gu (gushuying@tongji.edu.cn) or J. Ren (renjie6598@163.com).

Contract grant sponsor: National 863 Program of China; contract grant number: 2006AA02Z248.
Contract grant sponsor: Program for New Century Excellent Talents in University; contract grant number: NCET-05-0389.
Contract grant sponsor: Program of Shanghai Subject Chief Scientist; contract grant number: 07XD14029.
Contract grant sponsor: Shanghai International Cooperation of Science and Technology; contract grant number: 075207046.

modify the properties of many polymers with $CaCO_3$ by direct melt compounding such as polypropylene (PP), polyethylene, and so on. For PP/$CaCO_3$ and HDPE/$CaCO_3$, the preparation, mechanical properties, thermal properties, morphologies and viscoelastic properties have been extensively studied. $CaCO_3$, $CaSO_4$, talc, and other inorganic fillers were used to fill PLA. Most studies focused on the effect of the filler size, shape, size distribution, concentration and the dispersion in the PLA matrix on the mechanical properties, thermal properties, morphologies and fracture micro-mechanism of the composites.[13–21]

The rheological properties of filled polymers can not only characterize the nature of melt processability but also detect the internal structure of the composites. In the filler structure models, it has been widely accepted that when the particle loading is above percolation threshold, a secondary network structure will form.[22–28] Because of the interactions between the particles as well as particles and polymer matrix, there is either a particle–particle or particle–matrix "network" formation. Therefore, the filled polymers exhibited some particular rheological properties due to the different structures. A transition from liquid-like ($G'' > G'$) to solid-like response ($G' > G''$) at low frequencies was reported in poly (ethyl oxide)/silica nanocomposites due to the formation of a filler network.[29] Suspended particles tended to lead to agglomerates (soft flocks) or aggregates (hard agglomerates that require attrition to disintegrate) and played a very important role on the rheological properties of filled polymers. For example, Osman et al. found that the filler clusters strongly increased the moduli and viscosities of the composites, especially at low frequencies. G' increased much more than G''. The slopes of log $G'(\omega)$ and log $G''(\omega)$ in the terminal regime decreased.[30]

In this article, PLA/$CaCO_3$ composites with various filler content were prepared by melt-blending using a twin-screw extruder. The linear rheological behaviors of PLA/$CaCO_3$ were measured by dynamic measurements, whereas the nonlinear viscoelastic properties were measured by steady shear measurements. Our attention was focused on the rheological behaviors of PLA/$CaCO_3$ composites with different filler loading for the purpose of getting insight into the structure–rheological responses of the composites and providing useful information for the processability and the structures of the composites.

EXPERIMENTAL

Materials

PLA ($M_w = 180{,}000$, $M_w/M_n = 1.7$, L/D isomer ratio is 96 : 4, $T_g = 58°C$, $T_m = 155°C$) was supplied by Institute of Nano- and Bio-Polymeric Materials, Tongji University (Shanghai, China). Precipitated $CaCO_3$ (EMforce®, average major axis is 1.08 microns, average minor axis is 0.25 microns, and aspect ratio is 5.42) was supplied by Specialty Minerals Co. Ltd., USA.

TABLE I
Compositions of PLA/$CaCO_3$ Composites

Samples	PLA100	PLA90	PLA80	PLA70	PLA60
PLA (g)	100	90	80	70	60
$CaCO_3$ (g)	0	10	20	30	40

Sample preparation

PLA/$CaCO_3$ composites were prepared by melt-blending using a Leistritz twin-screw extruder with a screw diameter of 27 mm and an L/D ratio of 42. Before extrusion, PLA pellets were first dried at 60°C for 4 h and then dried at 100°C for 8 h under vacuum. $CaCO_3$ was dried at 80°C for 2 h under vacuum. The barrel temperatures during extrusion were set in the range of 165–185°C. The screw speed was set at 100 rpm and feed rate was 40 g min^{-1}. For better comparison, the neat PLA was also extruded under the same condition to keep identical thermal history with PLA/$CaCO_3$ composites. The formulations of the composites are shown in Table I. Samples for rheological measurements were prepared by hot compression molding under $\sim$ 5 MPa at 170°C for 3 min into 1-mm thick plates and then cut into 25-mm diameter parallel plates.

Morphology of PLA/$CaCO_3$ composites

The fractured surface morphology of PLA/$CaCO_3$ composites was observed by scanning electron microscopy (SEM) (Hitachi S-2360N). All samples were gold coated before observation. The SEM images were collected at an accelerating voltage of 15 kV.

Melt rheology

The rheological properties were measured by a strain-controlled rheometer advanced rheology expanded system (ARES) with a parallel plate geometry of 25-mm diameter plates. Dynamic oscillatory shear measurements were performed by applying a time dependent strain of $\gamma(t) = \gamma_0 \sin(\omega t)$ and the resultant shear stress is $\sigma(t) = \gamma_0[G'\sin(\omega t) + G''\cos(\omega t)]$, with G' and G'' being the storage and loss modulus, respectively. Measurements were conducted under ambient atmosphere with a sample thickness of 1–1.5 mm. Dynamic strain sweeps were carried out at 175°C and a frequency of 10 rad s^{-1} to determine the linear region of the melts. The linear

viscoelastic properties were observed by dynamic frequency sweep experiments. The strain amplitude was fixed at 1% to obtain reasonable signal intensities even at elevated temperature or low frequency and to avoid the nonlinear response. The measurements were performed in a frequency range of 0.1–300 rad s^{-1} and in the temperature range of 165–185°C. The master curves were generated using the principle of time temperature superposition and shifted to a common reference temperature (T_{ref}) of 175°C, which was chosen as the most representative of a typical processing temperature of PLA. Steady-shear viscosity measurements were conducted at 175°C using 25-mm diameter cone and plate geometry with a cone angle of 0.1 rad to investigate the nonlinear rheology of the melts. Shear rates were scanned from 0.1 to 100 s^{-1}.

For all the measurements, samples were dried in vacuum at 80°C for 12 h to remove water before testing and equilibrated for 10 min in the rheometer after loading at the desired temperature to remove the thermal history. All measurements were performed with a transducer capable of measurements over the range of 2–2000 g cm.

Statistical data analysis

Minitab statistical software package (Minitab 14) was used for multiple linear regression.

RESULTS AND DISCUSSION

Morphology of PLA/ $CaCO_3$ composites

SEM micrograph of the filler $CaCO_3$ is given in Figure 1. $CaCO_3$ is acicular and the particle size distribution is quite narrow. The fractured surface morphology was examined with SEM as shown in Figure 2. It is obvious that $CaCO_3$ particles are finely dispersed in the PLA matrix and no severe agglomeration is observed. For low-filler content samples (PLA90 and PLA80), the filler is almost embedded in the polymer matrix and no evident contact between $CaCO_3$ particles is observed. For high-filler content samples (PLA70 and PLA60), $CaCO_3$ particles contact with each other and a network structure between $CaCO_3$ particles forms. The network structure will result in some special rheological behaviors of the composites, which will be discussed further in the following sections.

Linear viscoelastic properties

To determine the linear viscoelastic limits of PLA and PLA/$CaCO_3$ composites melts, the dynamic strain sweep measurements were conducted at 175°C and a frequency of 10 rad s^{-1}. As shown in Figure 3, storage moduli (G') of the melts are independent on strain at low strain for all samples. The linear viscoelastic limits of PLA and low-filler content composites (PLA80, PLA90) are as high as about 100%. However, the linear viscoelastic limits of high-filler content composites (PLA60, PLA70) decrease sharply with the increasing of $CaCO_3$ content. G' drops sharply with increasing strain when the loading content reaches 30%. The linear viscoelastic limit of PLA60 extends only to a strain of about 2%. Therefore, the linear viscoelastic properties of PLA and its composites melts were conducted at a strain of 1%.

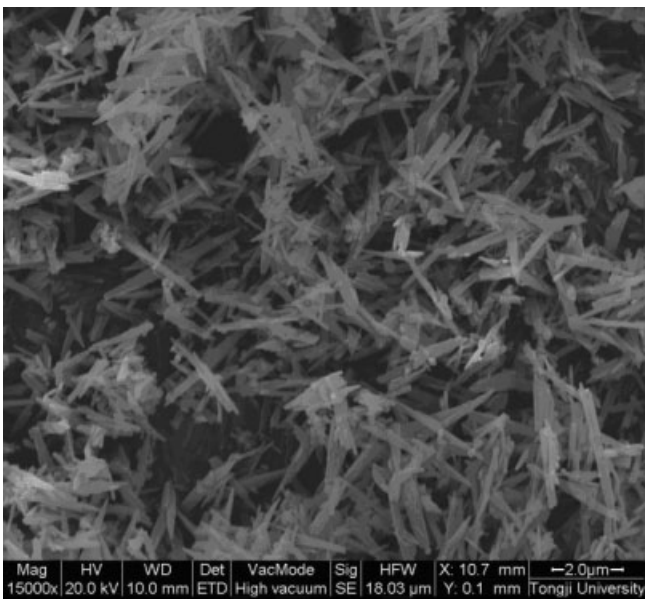

Figure 1 SEM micrograph of $CaCO_3$ filler.

The investigation of rheological properties of polymeric materials under molten state is crucial to gain a fundamental understanding of the nature of the processability and the structure-property relationship of these materials.[5] The rheological properties of polymeric materials were found to have a close relationship with the structures of copolymers[31,32] and polymer blends.[33] For polymer composites, rheology has also proven to be exquisitely sensitive to particle loading shape, size and distribution for a wide range of filler types.[34–38] Therefore, understanding the viscoelastic properties of polymer composites is of importance to get a fundamental knowledge of the process ability and the structure-property relationships of these materials.

The linear viscoelastic master curves for neat PLA and PLA/$CaCO_3$ composites melts (Fig. 4) were generated by the time-temperature superposition principle and shifted to a temperature (T_{ref}) of 175°C with both the frequency shift factor α_T and the modulus shift factor b_T. As shown in Figure 4, PLA/$CaCO_3$ composites melts with various filler contents show different viscoelastic behaviors. For low-filler content

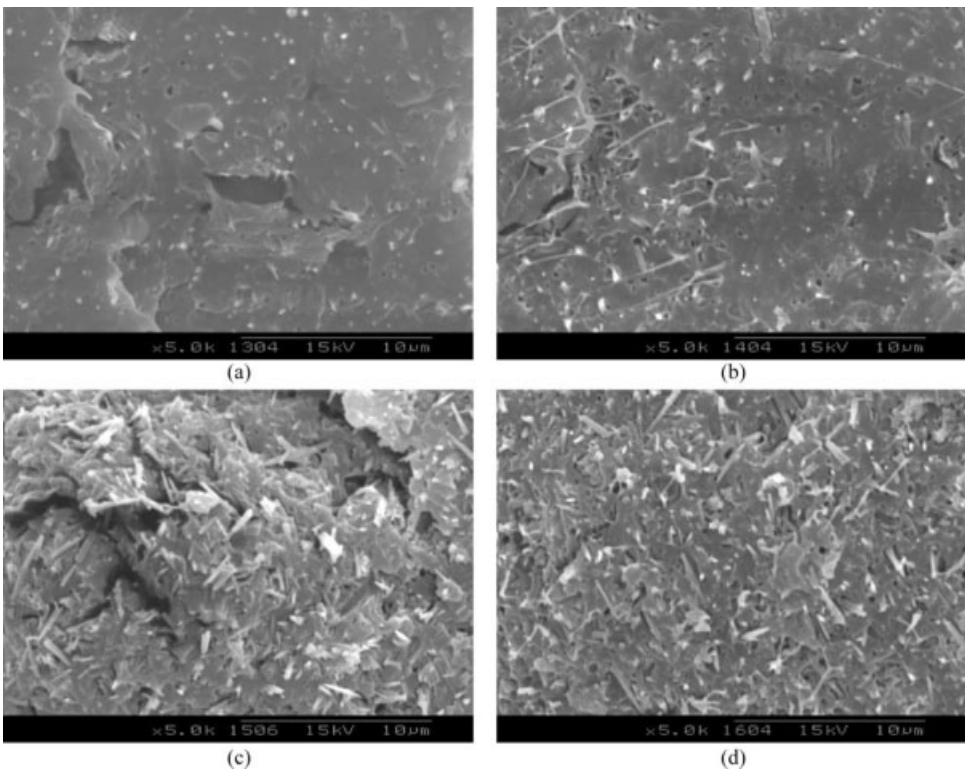

Figure 2 SEM micrographs of PLA/$CaCO_3$ composites: (a) PLA90; (b) PLA80; (c) PLA70; and (d) PLA60 (magnification ×5000).

samples (PLA90 and PLA80), the storage moduli $G'(\omega)$, loss moduli $G''(\omega)$, and complex viscosities η^* are lower than those of neat PLA at all frequencies. However for high-filler content composites (PLA70 and PLA60), the storage moduli $G'(\omega)$, loss moduli $G''(\omega)$, and complex viscosities $\eta^*(\omega)$ are several times higher than those of neat PLA at low frequencies. The result seems to be inconsistent with the results reported for nanocomposites. The moduli of nanocomposites generally increased with increasing filler loading at all frequencies.[5,6] Nevertheless according to the Payne effect,[39] it is generally accepted that the viscoelastic behaviors of filled polymers would be influenced by polymer matrix, the specific filler–PLA interaction and the filler network. When the content of $CaCO_3$ is low, it is insufficient to form a network [Fig. 2(a,b)] and the incorporation of the filler particles weakens the molecular interaction between the PLA segments. Therefore, the composites melts with low-filler content have lower $G'(\omega)$, $G''(\omega)$, and $\eta^*(\omega)$ than neat PLA. With increase of the filler content to the percolation threshold, filler particles begin to form a network through the interaction of filler–filler or filler-matrix as shown in Figure 2(c,d). The network causes higher $G'(\omega)$, $G''(\omega)$, and $\eta^*(\omega)$ of the melts. Similar results were obtained for nanoparticles dispersions and filled elastomers.[23,40]

On the other hand, the terminal behaviors of neat PLA, low-filled PLA and high-filled PLA composites show different behaviors. PLA is expected to shows characteristic homopolymer-like terminal flow behavior, expressed by the power laws $G'(\omega) \propto \omega^2$ and $G''(\omega) \propto \omega$ (i.e., terminal zone slopes of $G'(\omega)$ and $G''(\omega)$ are 2 and 1, respectively). The terminal

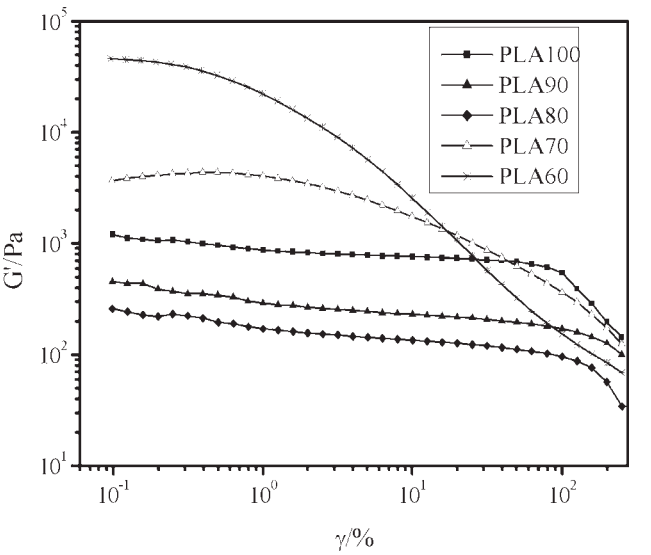

Figure 3 Dynamic strain sweep measurements of PLA and PLA/$CaCO_3$ melts at 175°C.

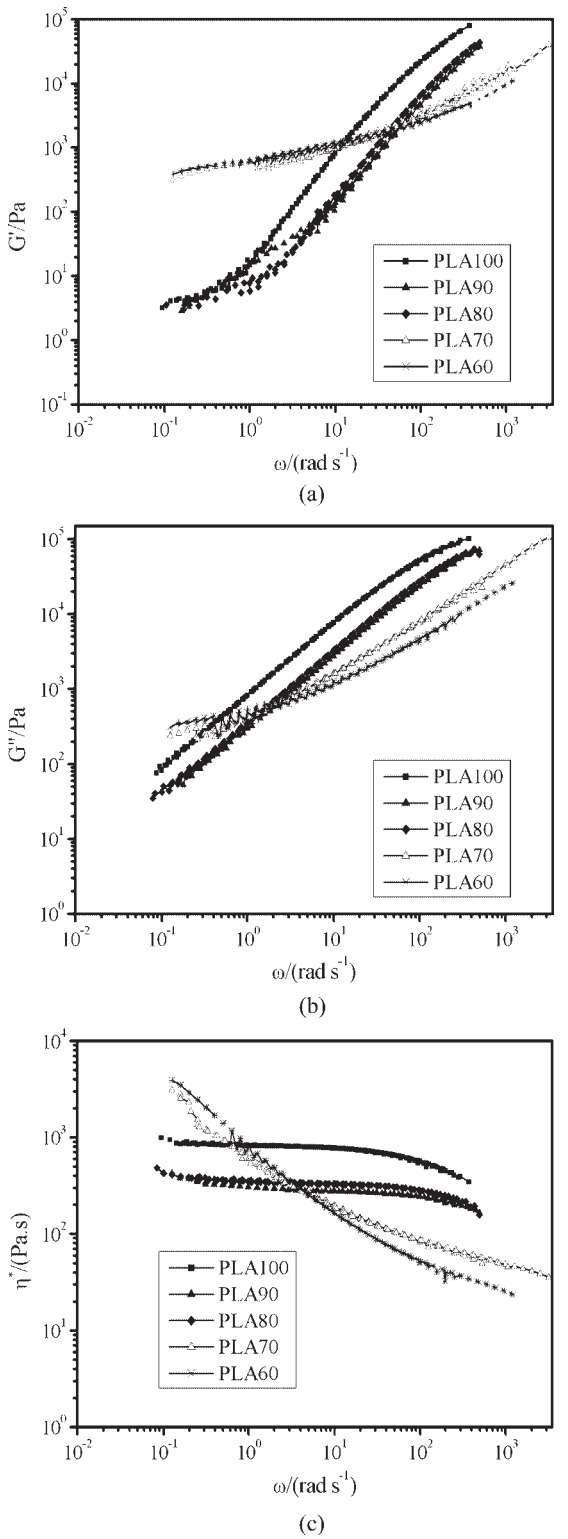

Figure 4 Reduced frequency dependence of storage moduli G' (a), loss moduli G'' (b), and complex viscosities η^* (c) of PLA and PLA/$CaCO_3$ composites melts (T_{ref} = 175°C).

zone slopes of PLA and PLA/$CaCO_3$ composites melts from the master curves for $G'(\omega)$ and $G''(\omega)$ at low frequencies ($\omega < 10$ rad s^{-1}) were calculated and presented in Table II. The slopes of $G'(\omega)$ and $G''(\omega)$ in the terminal region of PLA are 1.73 and 0.97, respectively, which are consistent with the results reported by Sinha Ray et al.[5] The slopes of $G'(\omega)$ for low-filled PLA/$CaCO_3$ composites melts are slightly lower than that of PLA and the slopes of $G''(\omega)$ are almost the same with that of PLA. However, the slopes of $G'(\omega)$ and $G''(\omega)$ for high-filled PLA/$CaCO_3$ composites decrease sharply when the content of $CaCO_3$ reaches 30%. The lower slope values and higher absolute values of dynamic moduli of high-filled PLA at low frequencies indicate the formation of network structures in PLA/$CaCO_3$ melts. In addition, there are also gradual changes of behavior from liquid-like to solid-like with increasing $CaCO_3$ content in PLA matrix, which is very common in the particle-filled polymers.

The master curves of dynamic complex viscosity $\eta^*(\omega)$ for PLA and PLA/$CaCO_3$ melts are shown in Figure 4(c). The complex viscosity $\eta^*(\omega)$ of neat PLA displays a Newton liquid behavior at low frequencies, which is constant with the frequency increasing up to 10 rad s^{-1}. The $\eta^*(\omega)$ of low-filled PLA shows the similar behavior with increasing frequency because of the major role of the interaction between the PLA molecular chain segments. Comparing PLA80 with PLA90, through 20% filler content in PLA80 does not lead to the formation of the network, some filler-matrix or filler–filler interaction occurs resulting in a slight increasing of viscosity. Therefore, the viscosity of PLA80 is a little higher than that of PLA90. On contrary, the $\eta^*(\omega)$ of high-filled composites shows stronger shear-thinning behavior at all measured frequencies and the tendency becomes stronger with increasing $CaCO_3$ content. The stronger shear-thinning tendency may be attributed to the destruction of the percolating network and the formation of the shear induced orientation of the dispersed $CaCO_3$ particles.

Flow activation energy

The dependence of the viscosity on temperature is one of the most important parameters to the processability of polymers. In a certain range of temperature, the dependence can be expressed in the Arrhenius form.[41]

$$\eta_0 = A\exp(E_a/RT) \quad (1)$$

Here, η_0 is the zero shear viscosity, R is the gas constant, A is a constant, and E_a is called the flow-activation energy. The higher the E_a is, the more temperature sensitive the melt is.

The flow-activation energy (E_a) values of neat PLA and PLA/$CaCO_3$ composites melts obtained from Arrhenius fit are presented in Table II. The values of

TABLE II
Rheology Characteristics of PLA and PLA/$CaCO_3$ Composites Melts

Samples	PLA100	PLA90	PLA80	PLA70	PLA60
Terminal region slopes of $G'(\omega)$	1.73	1.44	1.43	0.32	0.24
Terminal region slopes of $G''(\omega)$	0.97	0.98	0.97	0.59	0.49
E_a (kJ mol^{-1})	91.84	73.48	92.92	177.58	377.77

E_a were calculated by using η_0 data at the temperatures of 165, 170, 175, 180, and 185°C. For each calculation, the correlation coefficient (r^2) is better than 0.90. Standard deviations of residual (S) and P value are <0.1 and 0.05, respectively. The results obey Arrhenius model very well. Comparing with E_a of neat PLA, it is obvious that E_a tends to decrease with the incorporation of small amount of $CaCO_3$ and then increase sharply with increasing $CaCO_3$ content. E_a value of PLA60 (377.77 kJ mol^{-1}) is over four times of that of neat PLA (91.84 kJ mol^{-1}). This might be attributed to the formation of the network and the interaction between particle and particle or particle and matrix. On the other hand, the viscosity behaviors of PLA70 and PLA60 are much more sensitive to temperature. Therefore, the processing temperature for the high-filled composites should be strictly controlled.

Relaxation spectrum

The dependence of viscoelastic properties on time or frequency can be described by relaxation spectrum. The relaxation spectra (Fig. 5) of PLA and PLA/$CaCO_3$ composites were calculated from the master curves of G' in Figure 4(a) according to eq. (2) presented by Schwarzl.[42]

$$H_3'(\lambda) = \left[\frac{d^2}{d(\ln \omega)^2} - \frac{1}{4}\frac{d^3}{d(\ln \omega)^3}\right] G'(\omega)\Big|_{1/\omega=\lambda} \quad (2)$$

where $H_3'(\lambda)$ is the function of relaxation spectrum, λ is the relaxation time, $G'(\omega)$ is the function of dynamic storage modulus. The equation has proven to be useful to describe the relationship between the dynamic and transient moduli for homopolymers. Recently, the same relationship was successfully used to describe the viscoelastic properties of system with micelles dispersed in homopolymers[43,44] and nanocomposites.[36]

It can be concluded from Figure 5 that the dynamic viscoelastic response is a combination of the relaxation of macromolecular motions and the entanglements of polymer melts. However, there are some differences between the spectra of neat PLA and PLA/$CaCO_3$ composites. First, there is a distinct peak at $\lambda = 3.1$ s for neat PLA, whereas the peaks of PLA90, PLA80, PLA70, and PLA60 appear at $\lambda =$ 1.4, 0.08, 0.001, and 0.02 s, respectively. Second, plateaus appear in the relaxation spectra of PLA60, PLA70, and PLA80. Finally, $H(\lambda)$ spectra of PLA/$CaCO_3$ composites become higher than that of neat PLA after the peak. The peak at $\lambda = 3.1$ s for neat PLA as well as the peak at $\lambda = 1.4$ s for PLA90 might be caused by the movement of segment of PLA molecular chains. The peak of other samples might be caused by the destruction of the network in the PLA/$CaCO_3$ composites. The small amount of $CaCO_3$ weakens the interaction of PLA chains, which causes the lower $H_3'(\lambda)$ of PLA90 comparing with that of neat PLA. The network in the PLA/$CaCO_3$ composites with higher content of $CaCO_3$ increases the interaction between $CaCO_3$ particles as well as particle-matrix interaction. Therefore, the $H_3'(\lambda)$ spectra of PLA70 and PLA60 are higher than that of neat PLA.

Nonlinear viscoelastic properties

The steady shear rheological behavior of neat PLA and PLA/$CaCO_3$ composites are shown in Figure 6. At low-shear rates, the shear viscosities of PLA70 and PLA60 are higher than that of neat PLA. Nevertheless, the shear viscosities of PLA90 and PLA80 are lower than that of neat PLA. This is consistent with the results from dynamic frequency sweeps. On the other hand, the shear viscosities of PLA70

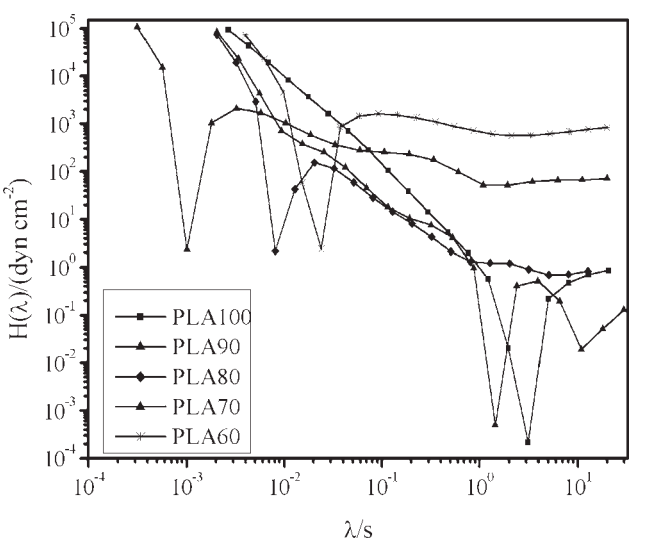

Figure 5 Relaxation spectra from master curves of neat PLA and PLA/$CaCO_3$ composites at 175°C.

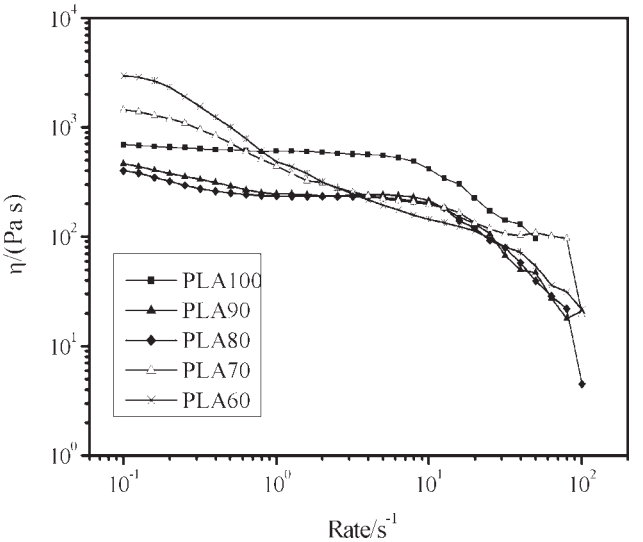

Figure 6 Steady shear viscosity of neat PLA and PLA/$CaCO_3$ composites as a function of shear rate at 175°C.

and PLA60 are lower than that of neat PLA at high-shear rates, which means PLA60 and PLA70 show stronger shear-thinning tendency.

To investigate the dependence of shear viscosity (η) on shear rate ($\dot{\gamma}$), the power law model was used to fit the non-Newtonian viscosity curves. The data fit in the power law equation well. All the equations have correlation coefficient (r^2) better than 0.99. All the P values are <0.0002. All the standard deviations of residuals are <0.04. The calculated values of flow index n for PLA100, PLA90, PLA80, PLA70, and PLA60 are 0.9252, 0.8481, 0.8816, 0.4912, and 0.3352, respectively. The results show that the increasing loading of $CaCO_3$ causes a dramatic decrease of n, which is in conformity with the more serious shear-thinning tendency caused by the destruction of the filler network. Although at low-shear rates the shear viscosities of PLA70 and PLA60 are several times higher than that of neat PLA, the incorporation of $CaCO_3$ can improve the processability at the shear rate from 1 to 60 s^{-1} because of the more serious shear-thinning tendency of high-filled PLA/$CaCO_3$ melts.

CONCLUSIONS

The fractured surface morphology and melt rheological properties of PLA/$CaCO_3$ composites were investigated. The results show that the $CaCO_3$ particles are evenly dispersed in the PLA matrix and no severe agglomeration is observed. The linear viscoelastic limits of PLA/$CaCO_3$ melts are smaller than that of neat PLA melt. The incorporation of low-content $CaCO_3$ (<20%) weakens the interaction between PLA chains segments and causes a reduction in the storage moduli, loss moduli, and dynamic viscosities. However, high-filled PLA/$CaCO_3$ composites (>30%) show obvious nonterminal behaviors. The lower slope values of $G'(\omega)$ and $G''(\omega)$ and higher absolute values of dynamic moduli indicate the formation of the percolating network structure in PLA/$CaCO_3$ melts. Furthermore, there is a significant increase in the E_a values when the $CaCO_3$ content is above 30%, which means that the viscosities of high-filled PLA composites are much more sensitive to temperature. Besides high-filled PLA composites show stronger shear-thinning tendency. The steady shear viscosities of high-filled PLA composites are much higher than that of the neat PLA at lower shear rates. At higher shear rates ($1\ s^{-1} < \dot{\gamma} < 60\ s^{-1}$), however, the shear viscosities of the high-filled PLA composites are lower than that of neat PLA as a result of the destruction of the percolating network.

References

1. Garlotta, D. J Polym Environ 2001, 9, 63.
2. Fang, Q.; Hanna, M. A. Ind Crop Prod 1999, 10, 47.
3. Sinha Ray, S.; Maiti, P.; Okamoto, M.; Yamada, K.; Ueda, K. Macromolecules 2002, 35, 3104.
4. Sinha Ray, S.; Okamoto, M. Macromol Mater Eng 2003, 288, 936.
5. Sinha Ray, S.; Yamada, K.; Okamoto, M.; Ueda, K. Polymer 2003, 44, 857.
6. Gu, S. Y.; Ren, J.; Dong, B. J Polym Sci Part B: Polym Phys 2007, 45, 3189.
7. Sivalingam, G.; Madras, G. Polym Degrad Stab 2004, 84, 393.
8. Chen, C. C.; Chueh, J. Y.; Tseng, H.; Huang, H. M.; Lee, S. Y. Biomaterials 2003, 24, 1167.
9. Pukanszky, B.; Fekete, E. Adv Polym Sci 1999, 139, 109.
10. Pukanszky, B.; Moczo, J. Macromol Symp 2004, 214, 115.
11. Rothon, R. N. Adv Polym Sci 1999, 139, 67.
12. Rothon, R. N. Particulate-Filled Polymer Composites. Rapra Technology, Ltd: Shrewsburg, UK, 2003.
13. Ma, C. G.; Mai, Y. L.; Rong, M. Z.; Ruan, W. H.; Zhang, M. Q. Compos Sci Technol 2007, 67, 2997.
14. Zuiderduin, W. C. J.; Westzaan, C.; Huetink, J.; Gaymans, R. J. Polymer 2003, 44, 261.
15. Avella, M.; Cosco, S.; Di Lorenzo, M. L.; Di Pace, E.; Errico, M. E.; Gentile, G. Eur Polym J 2006, 42, 1548.
16. Chan, C. M.; Wu, J. S.; Li, J. X.; Cheung, Y. K. Polymer 2002, 43, 2981.
17. Murariu, M.; Ferreira, A. D. S.; Degée, P.; Alexandre, M.; Dubois, P. Polymer 2007, 48, 2613.
18. Pluta, M.; Murariu, M.; Ferreira, A. D. S.; Alexandre, M.; Galeski, A.; Dubois, P. J Polym Sci Part B: Polym Phys 2007, 45, 2770.
19. Gorna, K.; Hund, M.; Vučak, M.; Gröhn, F.; Wegner, G. Mater Sci Eng 2007, 477, 217.
20. Urayama, H.; Ma, C.; Kimura, Y. Macromol Mater Eng 2003, 288, 562.
21. Osman, M. A.; Atallah, A. Macromol Chem Phys 2007, 208, 87.
22. Joshi, P. G.; Leonov, A. I. Rheol Acta 2001, 40, 350.
23. Donnet, J. B.; Bansal, R. C.; Wan, M. J. Carbon Black. Marcel Dekker: New York, 1993.
24. Cai, J. J.; Salovey, R. Polym Eng Sci 1999, 39, 1696.

25. Wang, Y.; Wang, J. J. Polym Eng Sci 1999, 39, 190.
26. Wang, Y.; Yu, M. J. Polym Compos 2000, 21, 1.
27. Wu, G.; Zheng, Q. J Polym Sci Part B: Polym Phys 2004, 42, 1199.
28. Xu, X.; Song, Y.; Zheng, Q.; Hu, G. J Appl Polym Sci 2007, 103, 2027.
29. Zhang, Q.; Archer, L. A. Langmuir 2002, 18, 10435.
30. Osman, M. A.; Atallah, A. Polymer 2006, 47, 2357.
31. Das, S.; Yilgor, I.; Yilgor, E.; Inci, B.; Tezgel, O.; Beyer, F. L.; Wilkes, G. L. Polymer 2007, 48, 290.
32. Arunn, A.; Gaymans, R. J. Polymer 2008, 49, 2461.
33. Zuo, M.; Zheng, Q. Macromol Chem Phys 2006, 207, 1927.
34. Cassagnau, P. Polymer 2008, 49, 2183.
35. Kelarakis, A.; Giannelis, E. P.; Yoon, K. Polymer 2007, 48, 7567.
36. Shen, L.; Lin, Y.; Du, Q.; Zhong, W.; Yang, Y. Polymer 2005, 46, 5758.
37. Wang, K.; Liang, S.; Peng, J.; Yang, H.; Zhang, Q.; Fu, Q.; Dong, X.; Wang, D.; Han, C. C. Polymer 2006, 47, 7131.
38. Hu, G.; Zhao, C.; Zhang, S.; Yang, M.; Wang, Z. Polymer 2006, 47, 480.
39. Payne, A. R.; Whittaker, R. E. Rheol Acta 1970, 9, 91.
40. Trappe, V.; Weitz, D. A. Phys Rev Lett 2000, 85, 449.
41. Ferry, J. D. Viscoelastic Properties of Polymers. Wiley: New York, 1980.
42. Schwarzl, F. R. Polymer-Mechanik. Berlin: Springer-Verlag, 1990.
43. Watanabe, H.; Yao, M. L.; Sato, T.; Osaki, K. Macromolecules 1997, 30, 5905.
44. Sato, T.; Watanabe, H.; Osaki, K.; Yao, M. L. Macromolecules 1996, 29, 3881.